Flow Separation Control on a NACA0012 Airfoil via a Porous, Compliant Coating

D. Venkataraman and A. Bottaro

DICAT, University of Genoa, 16145 Genoa, Italy

Abstract— **The purpose of this paper is to study the effect of a porous, compliant, anisotropic coating on the fluid-dynamical performance of a NACA0012 airfoil, under conditions of boundary-layer separation. This fluid-structure interaction problem is studied computationally in two dimensions by performing a detailed parametric study of the coating, with respect to its physical dimensions, characteristics and placement on the airfoil. Aerodynamic performances are quantified in terms of the non-dimensional mean drag and lift coefficients. The configuration described here is a separated flow at Re = 1100 and α = 70°. Coating parameters are found which decrease the amplitude of the drag oscillations by about 11% and increase the mean lift by about 9%.**

Keywords— **Fluid-structure interaction, flow-compliant feathers, weakly-coupled partitioned solver, immersed boundaries method, homogenized approach.**

I. Introduction

Optimization of flight performance has been an active research area for a number of years now – be it in terms of increasing the mean lift or optimization of fuel use achieved by decreasing the drag. Apart from its immediate implications in the commercial arena, these goals are also sought while designing unmanned aerial vehicles (UAVs), and micro aerial vehicles (MAVs), which are used for a variety of civil and military operations.

In this research, to achieve the goal of enhancing aerodynamic performances, inspiration is taken from bird and insect flight. Birds, typically during the gliding and landing phases, increase the surface area of their wings by means of "morphing" or shape optimization – both passive and active. Passive flow separation control is realized here by means of the "pop-up" of flow-compliant feathers on the wings, which can passively adapt to the flow [1,2]. This deformable layer is capable of storing and then releasing energy in the boundary layer, according to the instantaneous fluid flow. Consequently, this affects the vortex shedding and explains the efficient flight of birds under conditions of high angles of attack or in gusty winds. Passive shape adaptation of the fluid-dynamic configuration has the added commercial advantage of not requiring any additional energy input to achieve the objective of high lift or low drag.

The present fluid-structure interaction problem is solved computationally in two dimensions with a partitioned approach, by dividing the computational domain into three parts – the airfoil, the porous layer of "pop-up feathers" and the fluid. Instead of using a body-fitted dynamic mesh, a stationary Cartesian mesh – fine near the airfoil and sparse far away from it, is used (which consequently saves computational cost) by employing the immersed boundary method [3]. Besides being porous to fluid flow, the coating is also anisotropic and compliant. These properties realistically model birds' feathers, by accounting for the ability of the fluid to be oriented along a particular direction as it enters the layer as well as the ability of the layer to deform according to the local flow. Further, this continuum of feathers is approximated homogeneously by a discrete number of reference feathers, each of these being surrounded by a control volume of given porosity. Beginning with an initial condition for the fluid variables and the reference feathers, the computation is done in an iterative loop as follows:

1. The Navier-Stokes equations with forcing are solved by DNS using the immersed boundaries method.
2. Fluid to structure forcing is computed, with the solution of the fluid variables obtained in the previous step.
3. A non-linear equation (which governs the structures' dynamics) with forcing from the last step is solved for each reference feather.
4. Structure to fluid forcing is computed.

Between each of the steps of the partitioned solver given above, weak coupling is assumed. Some details of these steps are outlined in section II.

II. Numerical method

The fluid velocity and pressure are initialized to the free-stream velocity and zero, respectively. The initial configuration of the reference feathers is initialized to the equilibrium angle about which each of these oscillate while their velocities are initialized to zero. Control volumes are defined symmetrically about each of these reference feathers. A non-dimensional variable called *packing density* φ is introduced, which gives the ratio of volume occupied by the feathers to the total volume. This parameter captures the non-homogeneous nature of the dense coating, approximated by a discrete number of feathers. Then the following loop is executed in time.

C.T. Lim and J.C.H. Goh (Eds.): WCB 2010, IFMBE Proceedings 31, pp. 52–55, 2010.
www.springerlink.com

Fluid Solver: The direct numerical simulation of the unsteady incompressible Navier-Stokes equations is performed, using the feedback forcing formulation of the immersed boundaries method [3]. A buffer zone is introduced at the end of the computational domain to damp the unsteady structures in the wake of the airfoil, before they reach the end of the domain. To account for the presence of these immersed boundaries (airfoil and buffer zone) and the forcing from the structure onto the fluid, the Navier-Stokes equation has a volume force term $\boldsymbol{F}$ given (as in [4]) by:

$$\boldsymbol{F} = \boldsymbol{F}^a + \boldsymbol{F}^b + \boldsymbol{F}^h \quad (1)$$

where $\boldsymbol{F}^a$ and $\boldsymbol{F}^b$ are respectively the immersed boundary forces due to the airfoil and the buffer zone, which respectively force the velocity on the airfoil and buffer boundaries to converge to *zero* and to the *free-stream velocity*. $\boldsymbol{F}^h$ is the force due to the feathers on the fluid (initialized to zero in the first time step). The Navier-Stokes equations are solved, using staggered flow variables, by a predictor-corrector scheme, with an explicit Adams-Bashforth scheme for the convective part, a semi-implicit Crank-Nicolson scheme for the viscous part and a conjugate gradient algorithm for the resolution of the Poisson pressure equation.

Fluid to Structure Forcing: The normal component of the forcing from the fluid onto the structure $\boldsymbol{F}_n^h$ is computed, by Koch & Ladd's formulation [5], while the tangential component $\boldsymbol{F}_t^h$ is derived using a Stokes approximation [4]. The total force $\boldsymbol{F}_{i,j}^h$ for each grid point with index *(i,j)* is transferred to each reference feather, by first integrating it over the control volume surrounding it. The force on each reference feather is now denoted by $\boldsymbol{F}_k^h$, where *k* is the index of a generic reference control element.

Structure Solver: The dynamics of each reference feather, each of which is modeled as a rigid beam oscillating about an equilibrium angle, is governed by the effects of inertia, rigidity, interaction and losses, out of which the effect of rigidity is taken predominant. The angular displacement θ for each reference feather is solved by a non-linear equation, given in non-dimensional form (as in [4]) by:

$$\ddot{\theta} + \gamma\dot{\theta} + f_1(\theta) + \kappa f_2(\theta) = \mu_{ext}(t_c^*) \quad (2)$$

using explicit 4-step Runge-Kutta method. Here, γ is the ratio between the frequencies corresponding to the losses and rigidity effects, κ is the square of the ratio between the frequencies corresponding to the interaction and rigidity effects, f_1 and f_2 are non-linear functions modeling the moments of rigidity and interaction respectively, and μ_{ext} is the fluid to structure momentum forcing on a reference feather (made non-dimensional by a rigidity term).

Structure to Fluid Forcing: The positions and velocities of the control volumes are interpolated from those of the reference feather that each of them surrounds, using the packing density φ. The normal and tangential components of the forcing onto the fluid are computed as done before in the fluid to structure forcing step.

During each iteration, the instantaneous non-dimensional drag and lift coefficients are calculated and the final aerodynamic performance is quantified by the time-averaged drag and lift coefficients.

III. Results

The case of the NACA0012 airfoil without the compliant coating is first considered. Simulations are done for different angles of attack of the airfoil, varying from 0° to 90°, for a chord-based Reynolds number equal to 1100. A steady drop in the lift coefficient is observed after an angle of 48°, as also illustrated in the paper by Soueid et al. [6].

To illustrate the results in the after-stall regime, we focus on an angle of attack equal to 70°. The lift and drag coefficients, for the airfoil without and with control elements, are plotted as functions of time in Fig. 1. Time is rendered dimensionless with the free stream speed and the chord length. In the case without control, two distinct frequencies in the spectrum – a large one (equal to 1.204) and a small one (equal to 0.147) – are observed in both the signals. In Fig.2, color plots of the pressure field near the airfoil (in the cases without and with control) at four different time instants within a period of the time signals, are shown.

To achieve optimal fluid-dynamical performance, we try to synchronize the time scales of the fluid and the structure. Since the frequency scale of rigidity is predominant over the other two frequency scales of interaction and losses, the goal is to identify the "right" coefficient of rigidity of the control elements. This is accomplished by testing different coatings with characteristic rigidity frequencies varying between the high and low frequencies of the case without control, referred to above.

In accordance with the linear stability analysis of equation (2) carried out by Favier et al [4], to achieve asymptotic stability of the fluid-structure system, a small value of γ (equal to 0.05) is chosen. This fixes the value of the dissipation parameter of the control, corresponding to each modulus of rigidity to be tested. The interaction parameter for all the cases is chosen to satisfy the constraint:

$$\omega_I < \omega_s < \omega_r \quad (3)$$

where ω_r, ω_s and ω_I are the characteristic structural frequencies due to rigidity, interaction and dissipation effects, respectively.

For the present study, the placement of the coating and the packing density are fixed. In particular, the coating occupies about 70% of the area of the airfoil suction side, a little away from the leading edge, and the packing density φ is chosen equal to 0.0085; Furthermore, the initial ("equilibrium") position of the reference feathers is parallel to the free-stream. For a characteristic rigidity frequency equal to 0.477, there is an increase in the mean lift by 9.33% and a decrease in the fluctuations of the drag coefficient by 10.75% (whereas the mean drag remains roughly constant).

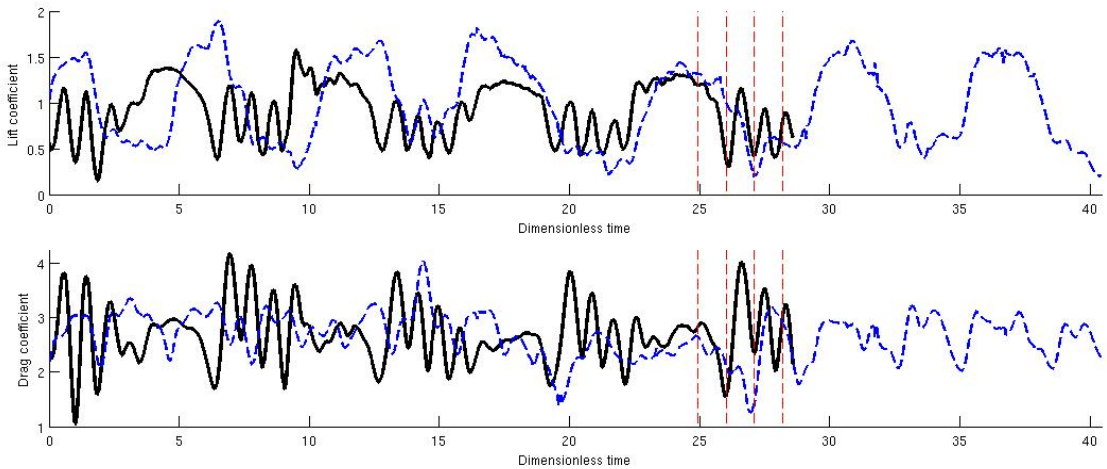

Fig. 1 Aerodynamic coefficients for smooth airfoil (solid lines) and airfoil with coating (dashed lines). The figure on the top shows the lift coefficient while the figure on the bottom shows the drag coefficient, both as functions of dimensionless time

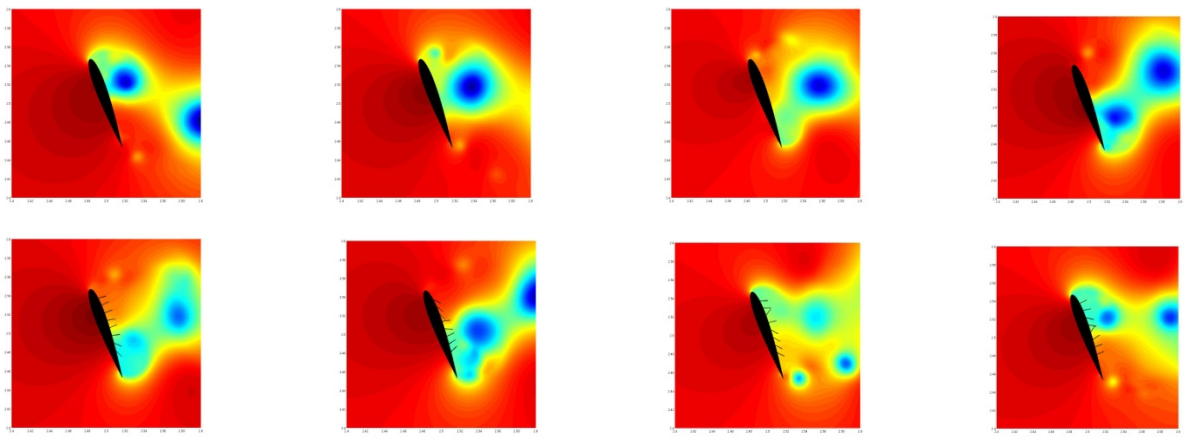

Fig. 2 Plots of pressure field near the airfoil for the case without control (top) and with control (bottom) at four instants of time (marked by vertical dashed lines in Fig. 1) chosen roughly within a period of oscillation of the lift and drag signals in the uncontrolled case

IV. Physical interpretation

By comparing the time signals of the drag and lift coefficients for a smooth airfoil and one with control (as shown in Fig.1), it can be seen that the dynamics in the presence of the coating retains the low frequency component present in the signals. This phenomenon can be attributed to a "lock-in" effect in which the coating synchronizes onto a frequency close to the natural frequency of the fluid system [7].

The effect of the control elements appears on the pressure and velocity fields. By observing the pressure field near the airfoil (as shown in Fig.2), it is found that the pressure on the suction side of the airfoil with the compliant coating is larger as compared to the uncontrolled case. This results in enhanced lift and reduced drag fluctuations.

Further, the control elements are responsible for the creation of smaller coherent vortices behind the airfoil, which are, on the average, further away from the suction side and less intense, as opposed to a smooth airfoil case. It can also be observed from inspection of the velocity field (not shown here) that the coating produces a layer of low-velocity fluid on the suction side which opposes separation, instant-by-instant.

V. Conclusions

We have numerically studied the passive control of flow separation on a symmetric airfoil using a dense coating, as a fluid-structure interaction problem. The inspiration for this has been the observation of the pop-up of covert feathers in birds during landing approaches or in gusty winds. The coating used here has properties able to affect the topology of the flow in the proximity of the rear of the airfoil – namely, porosity, anisotropy and compliance. The numerical treatment is based on a weakly-coupled partitioned solver [4].

It is found by a numerical parametric analysis that such a coating is capable of improving the aerodynamic performances of the immersed body, by adapting to the separated flow. The coating modifies the vortex shedding process, hence contributing to enhanced performances. This is achieved by a synchronization of the oscillations of the structures onto a frequency close to the natural frequency of the fluid system.

A set of control parameters has been found which causes the mean lift to increase by more than 9% and the drag fluctuations to decrease by more than 10%. Other simulations are under way to identify optimal structural parameters.

Finally, we envision to employ the continuum field theory of Gopinath & Mahadevan [8] based on the equations of poroelasticity to model realistic layers in three-dimensions and characterize rigorously the material properties of various types of coatings which are found to be efficient in managing the fluid flow.

References

1. Bechert D W, Bruse M, Hage W, Meyer R (1997) Biological surfaces and their technological application-laboratory and flight experiments on drag reduction and separation control. AIAA J 97:1960–1997.
2. Schluter J U (2009) Lift enhancement at Low Reynolds Numbers using Pop-Up Feathers. AIAA J. Aircraft 47 (1): 348.
3. Fadlun E A, Verzicco R, Orlandi P, Mohd-Yusof J (2000) Combined Immersed-Boundary Finite-Difference Methods for Three-Dimensional Complex Flow Simulations. J. Comput. Phys. 161:35–60.
4. Favier J, Dauptain A, Basso D, Bottaro A (2009) Passive separation control using a self-adaptive hairy coating. J. Fluid Mech. 627: 451-483.
5. Koch D L & Ladd J C (1997) Moderate Reynolds number flows through periodic and random arrays of aligned cylinders. J. Fluid Mech. 349: 31-66.
6. Soueid H, Guglielmini L, Airiau C, Bottaro A (2009) Optimization of the motion of a flapping airfoil using sensitivity functions. Comput. Fluids 38: 861-874.
7. De Langre E (2006) Frequency lock-in caused by coupled-mode flutter. J. Fluids Struct. 22 (6-7):783-791.
8. Gopinath A, Mahadevan L (2010) Elastohydrodynamics of wet bristles, carpets and brushes. Submitted to Proc. Royal Soc. A.

Author: Divya Venkataraman
Institute: DICAT, University of Genoa
Street: Via Montallegro 1, 16145
City: Genoa
Country: Italy
Email: divya@dicat.unige.it